Integrative Biology
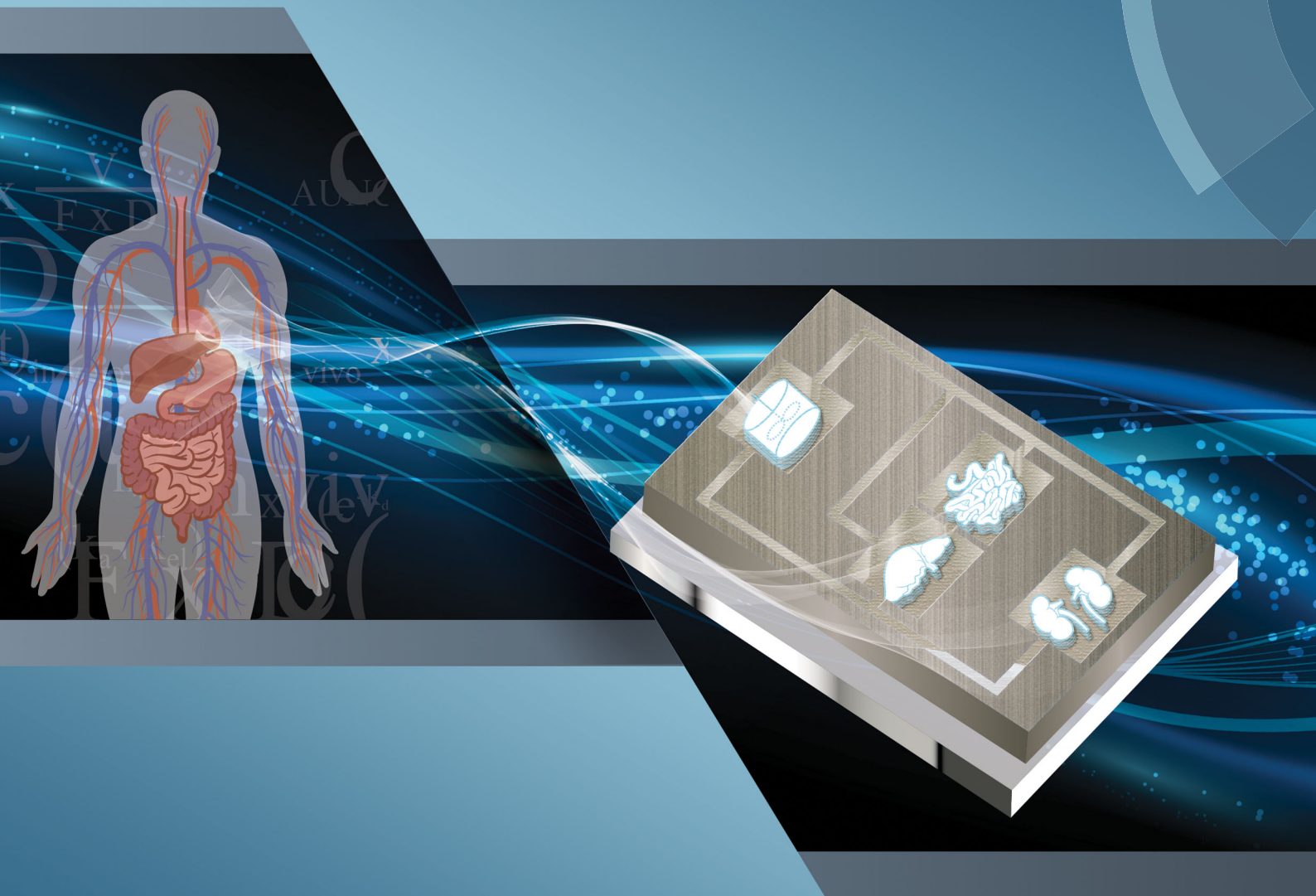
Interdisciplinary approaches for molecular and cellular life sciences

rsc.li/integrative-biology

ROYAL SOCIETY OF CHEMISTRY

PAPER
Murat Cirit *et al.*
Multi-functional scaling methodology for translational pharmacokinetic and pharmacodynamic applications using integrated microphysiological systems (MPS)

Indexed in Medline!

PAPER

Multi-functional scaling methodology for translational pharmacokinetic and pharmacodynamic applications using integrated microphysiological systems (MPS)†

Christian Maass,[a] Cynthia L. Stokes,[b] Linda G. Griffith[a] and Murat Cirit*[a]

Microphysiological systems (MPS) provide relevant physiological environments *in vitro* for studies of pharmacokinetics, pharmacodynamics and biological mechanisms for translational research. Designing multi-MPS platforms is essential to study multi-organ systems. Typical design approaches, including direct and allometric scaling, scale each MPS individually and are based on relative sizes not function. This study's aim was to develop a new multi-functional scaling approach for integrated multi-MPS platform design for specific applications. We developed an optimization approach using mechanistic modeling and specification of an objective that considered multiple MPS functions, *e.g.*, drug absorption and metabolism, simultaneously to identify system design parameters. This approach informed the design of two hypothetical multi-MPS platforms consisting of gut and liver (multi-MPS platform I) and gut, liver and kidney (multi-MPS platform II) to recapitulate *in vivo* drug exposures *in vitro*. This allows establishment of clinically relevant drug exposure–response relationships, a prerequisite for efficacy and toxicology assessment. Design parameters resulting from multi-functional scaling were compared to designs based on direct and allometric scaling. Human plasma time–concentration profiles of eight drugs were used to inform the designs, and profiles of an additional five drugs were calculated to test the designed platforms on an independent set. Multi-functional scaling yielded exposure times in good agreement with *in vivo* data, while direct and allometric scaling approaches resulted in short exposure durations. Multi-functional scaling allows appropriate scaling from *in vivo* to *in vitro* of multi-MPS platforms, and in the cases studied provides designs that better mimic *in vivo* exposures than standard MPS scaling methods.

Insight, innovation, integration

Microphysiological systems provide relevant physiological environments *in vitro* for studies of pharmacokinetics, pharmacodynamics and biological mechanisms for translational research. Designing multi-MPS platforms is essential to study multi-organ systems. There is an immediate need for a mechanistic approach to design multi-MPS platforms. Common approaches for MPS scaling (sizes, volumes and flow rates) are direct miniaturization and allometric scaling. These empirical approaches consider each MPS individually and are based on physical size. Subsequently, integrated multi-MPS platforms are built by simply connecting individually developed MPSs together. In this work, a novel multi-functional scaling approach is introduced to design integrated multi-MPS platforms, which is adaptable to various research interests, *e.g.* different MPS types or arrangements and study objectives (pharmacokinetics, pharmacodynamics, disease models).

1. Introduction

Over the last decade, development of microphysiological systems (MPS) aiming to represent relevant human physiology and organ-specific functions *in vitro* has accelerated, in part driven by federal funding agency initiatives in the United States and internationally.[1–3] Numerous individual MPSs have been developed to represent specific organs or sub-organ systems, including liver, kidney, lung, muscle, cardiac and skin,[4–10] and multi-MPS platforms with interconnected MPSs are also being developed to capture multi-organ physiology.[11–14]

The vision is for MPS technologies to provide improved *in vitro* tools and increased translational success for pharmacokinetic,

[a] Department of Biological Engineering, Massachusetts Institute of Technology, Cambridge, USA. E-mail: mcirit@mit.edu

[b] Stokes Consulting, Redwood City, USA

pharmacodynamic, toxicology and biomarker discovery applications.[15–18] Results from current *in vitro* models as well as animal models frequently differ from early clinical trial results, and appropriately designed MPSs will most likely represent *in vivo* tissue and organ biology more adequately. This in turn should provide improved preclinical tools to guide decision-making with regards to drug efficacy and patient safety in clinical trials, as well as potentially informing early disease modeling for complex or systemic diseases.

Within an MPS device, the cell types included, micro-architecture for cell culture, fluid flow rates, and culture protocol work synergistically together to mimic desirable features of the 3D structure, mechanical strain and flow shear stress[5] found *in vivo*. For interconnected MPSs, design parameters (*e.g.* tissue sizes, medium volumes) and operational strategies (*e.g.*, flow partitioning, flow rates) need to be specified to reproduce desired biological functions within practical constraints, and in consideration of the applications (*i.e.*, the systems-level biological phenomena of interest). The most appropriate design approach for MPSs interacting on a fluidic platform at a systems level continues to be debated. The specific applications of a single or multi-MPS platform (*e.g.* drug pharmacokinetics, specific pharmacodynamics, toxicology or biomarker discovery) will likely drive design, since it is unlikely that a single design will be appropriate for all applications.

Common scaling approaches to date include direct miniaturization and allometric scaling of a variety of *in vivo* physical characteristics such as organ/tissue mass, blood flowrates, volumes and residence times.[1,11,19,20] The focus of these approaches is to preserve the relative biomass scales of each organ (*e.g.* blood volume to flow rate, or volume to mass ratios). These methodologies result in one design for single- or multi-MPS platforms, which is independent of the study application. Therefore, it is widely acknowledged that more function-based scaling is desirable.[19,21–23]

Functional scaling aims at recapitulating selected *in vivo* physiological processes or functions in the *in vitro* environment (*e.g.* an MPS). The idea is to determine design parameters for single MPSs or multi-MPS platforms by considering functions of MPSs relevant to the application or study objective of interest. These designs would be based upon recapitulating the functions rather than relative masses, flow rates, and similar, the typical considerations in direct or allometric scaling approaches.

Examples of biological functions to be considered in functional scaling might be drug metabolism and excretion (for pharmacokinetic and pharmacodynamic applications), insulin production, and glucose metabolism rates (for diabetes studies), or cytokine production rates and concentrations (for inflammation studies).

A mechanistic modeling approach would provide an appropriate framework as it allows consideration of each MPS function and characteristics of an integrated multi-MPS platform simultaneously. Further, as any individual MPS seldom replicates every feature of the organ *in vivo*, application-driven design of MPS components to capture essential features for the application is crucial to create a relevant physiological and pharmacological environment.[1,2,19,21,24]

Several multi-MPS platforms[11,19] have been developed by interconnecting existing single-MPSs. While the MPSs in such systems are typically on the same approximate physical scale as each other, each has usually been developed independently and the interconnections were limited by practical considerations (*e.g.*, ease of handling, pumping constraints, *etc.*). A recent theoretical study introduced a quantitative approach to multi-MPS design and data analysis. The authors investigated sensitivity and impact of design parameters (*e.g.* medium volumes or flow rates) in an integrated four-MPS system on pharmacologically relevant metrics for drug concentration and distribution.[13] However, a method to simultaneously consider multiple MPS functions as the basis for specifying MPS design and guiding multi-MPS operations is still needed. Such an approach requires consideration of functions from each MPS as well as integrated MPS function simultaneously.

The aim of this work is to develop and demonstrate feasibility and applicability of a multi-functional scaling approach to inform the design of study-specific, integrated, multi-MPS platforms. A novel multi-functional scaling framework was developed based on mechanistic modeling of the biological mechanisms, specification of an objective function, and identification of design parameters (those, which would be specified in order to optimize the objective function). As use cases, two multi-MPS platforms (gut–liver and gut–liver–kidney) were investigated computationally, focusing on pharmacological applications using available preclinical and clinical data. To evaluate our approach, we test how well our designed multi-MPS platforms recapitulate drug exposure of additional drugs not used in the initial multi-MPS platform design by comparing predicted exposures in the theoretical *in vitro* platform to known *in vivo* exposures. Recapitulating relevant exposures *in vitro* is important to establish exposure–response relationships, which describe a response or an effect in the body or an organ of interest due to the drug over time.[25] These relationships provide a foundation for further studies of efficacy and toxicology in a more clinically-relevant manner, as well as a means to identify potentially safe and hazardous dosing regimens for drugs.

In addition, we compare our scaling approach to results from designing the two multi-MPS platforms using the traditional methods of allometric scaling and direct scaling. We find that our multi-functional scaling methodology can provide system designs that should recapitulate relevant *in vivo* drug exposures *in vitro*.

2. Materials and methods

The goal of the application-specific design for a hypothetically integrated multi-MPS system was to recapitulate human drug exposures *in vitro*. Two different multi-MPS platforms – gut–liver MPS platform (multi-MPS platform I) and a gut–liver–kidney MPS platform (multi-MPS platform II) – were investigated. Three different scaling approaches to design multi-MPS platforms were applied: (i) multi-functional scaling, (ii) direct scaling, and (iii) allometric scaling.

In general, the multi-functional scaling algorithm consists of (1) mathematical models of the biological mechanisms of each MPS and integrated multi-MPS platform, (2) specification of known or desired model parameters (both biological and operational), (3) specification of an objective function that embodies the critical MPS platform biological functions of interest and the selection of related, available experimental data to be used in the optimization process, (4) selection of design parameters – operational parameters to be estimated by minimizing the objective function, (5) specification of constraints for design parameters, and (6) assessment of design outcome by evaluating a metric related to the objective function and biological functions of the platform.

The details of the scaling approaches and mathematical equations are included in our descriptions of the two multi-MPS platform test cases below as well as in Supplement S1 (ESI†).

All simulations and parameter estimations were performed in Matlab (R2016a, The MathWorks, Inc., Natick, Massachusetts, United States).

In contrast, the general workflow for direct and allometric scaling to determine design parameters consists of steps (1) and (2) as described above, (3) calculation of design parameters by applying a scaling factor or a power-law equation, and (4) evaluation of design outcome by the same metric.

Computational investigation of multi-MPS designs

The application focus of the two multi-MPS platforms we investigated is pharmacokinetics following oral administration of drugs. Both platforms were mathematically described by a set of ordinary differential equations.

The first multi-MPS platform investigated comprises gut and liver MPSs plus a mixing chamber (Fig. 1(a)), to capture the basic processes of drug absorption, metabolism and distribution in a closed-loop system. The systemic circulation flow rate (Q_{sys}) distributes cell culture medium and drugs between the mixing chamber and the MPSs. Flow partitioning to each MPS was based on physiological partitioning of cardiac output for liver (hepatic artery) and gut (portal vein).[26,27] Drugs can be administered either to the mixing chamber (representing intravenous (IV) administration) or the apical site of the gut MPS (representing oral administration). For the latter, permeability constants (P_{gut}) of various drugs for transport through CaCo-2 cell monolayers, a typical gut epithelium model, were obtained from the literature and are used in the model. Drug is assumed to be metabolized in the liver MPS by hepatocytes only. Both parent drug and metabolites are distributed by flow among the mixing chamber, gut and liver. Intrinsic clearance rates (Cl$_L$) for parent drugs by hepatocytes *in vitro* were obtained from literature reports for suspension hepatocyte cultures.

The second multi-MPS platform investigated is a semi-closed system comprising gut, liver, kidney MPSs and a mixing chamber (Fig. 1(b)) to additionally include excretion and reabsorption processes *via* the kidney MPS. The features of the gut and liver MPSs are the same as in multi-MPS platform I. The flowrate to the kidney MPS (Q_{kid}) is estimated relative to the physiological flows *in vivo* to gut and liver.[27] This flow is divided between the
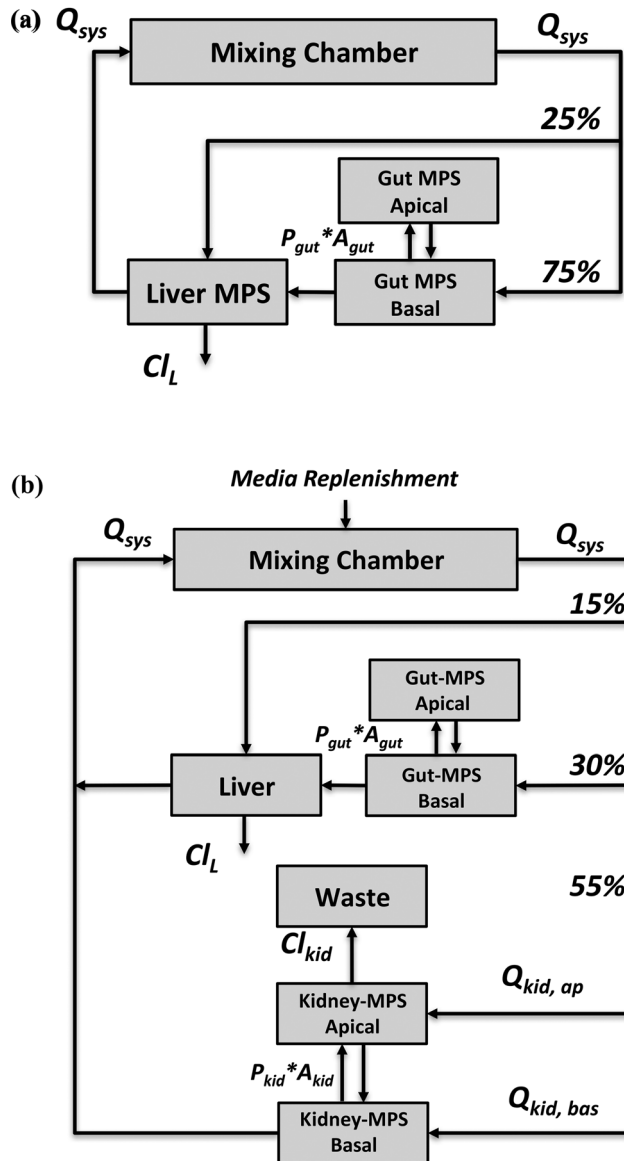

Fig. 1 Schematic overview of (a) a gut–liver-mixing chamber platform (multi-MPS platform I) and (b) a gut–liver–kidney-mixing chamber platform (multi-MPS platform II). Three scaling approaches were investigated to determine design (*i.e.* model) parameters and checked for their feasibility to satisfy the study objective. Q_{sys} = systemic flow rate, Q_{kid} = flow rate to kidney, P_i = permeability, A_i = surface area, Cl_i = clearance; L = liver, kid = kidney.

renal lumen ($Q_{kid,ap}$) and the interstitium ($Q_{kid,bas}$). Reabsorption rates from lumen to interstitium as well as secretion rates from interstitium to lumen were obtained from *in vitro* permeability studies using renal proximal epithelial cells (MDR1-MDCK). To recapitulate excretion of parent drug from the kidney MPS, a constant flow to a waste container (Q_{waste}) was introduced and set equal to the renal luminal flow ($Q_{kid,ap}$). As no active filtration between medium and drug occurs, medium was replenished at the same rate as the excretion rate (Q_{waste}) to the mixing chamber (media replenishment).

Mechanistic models using ordinary differential equations were implemented for each of the platforms to describe absorption,

distribution, metabolism and excretion of a compound and their effects on that compound's time–concentration profile in the integrated MPS platform *in silico* (see Supplement S1, ESI†).

MPS scaling using three approaches

Multi-functional scaling. The novel multi-functional scaling algorithm described above was used to inform the design of these integrated MPS platforms of interest.

Training sets of eight drugs for each platform (Tables 1 and 2) were used to identify design parameters. In the algorithm, the objective function is a weighted squared difference between a model outcome and corresponding measurements:

$$\text{Objective function} = \min\left(\frac{\text{prediction} - \text{observation}}{\text{prediction}}\right)^2 \quad (1)$$

where prediction is the model outcome and observation corresponds to the clinical data for the study objective.

More specifically, in multi-MPS platform I, the study objective was to recapitulate clinically observed plasma concentration profiles (observation) of each drug from the training set in the mixing chamber (prediction) using model calculations of the drug concentration profile in the mixing chamber. In multi-MPS platform II, the study objective included two elements, recapitulating the plasma concentration profiles as done in multi-MPS platform I and to recapitulate the fraction excreted parent drug in humans (observation) in the waste container (prediction, Fig. 1(b)) of the platform. For each platform, the information was simultaneously modeled to yield a single set of design parameters based on all eight drugs.

To account for the dose and bioavailability differences of drugs *in vivo*, the *in vivo* time–concentration profiles were normalized as follows:

$$c(t)_{in\,vivo}{}' = c(t)_{in\,vivo} \times \frac{V}{F \times D} \quad (2)$$

$$c(t)_{in\,vivo} = \frac{F \times D}{V} \times \frac{k_a}{(k_a - k_{el})} \times \left(e^{-k_{el} \times t} - e^{-k_a \times t}\right) \quad (3)$$

where $c(t)_{in\,vivo}$ is the measured time-dependent drug plasma concentration, $c(t)_{in\,vivo}{}'$ is the normalized drug concentration, F is bioavailability, D is administered dose, V is the volume of distribution, k_a is the absorption rate constant, k_{el} is the elimination rate constant, and t is time. Eqn (3) is based on the standard ordinary differential equation for the time-dependent plasma concentration profile *in vivo* in a one-compartmental model with first-order oral absorption and metabolism after a single dose.

To compare the *in vitro* platform response to the normalized *in vivo* time–concentration profiles, the same conceptual normalization was performed for the model concentration:

$$c(t)_{in\,vitro}{}' = c(t)_{in\,vitro} \times \frac{V_{in\,vitro}}{F_{in\,vitro} \times D_{in\,vitro}} \quad (4)$$

where $V_{in\,vitro}$ is the total media volume of the platform, $D_{in\,vitro}$ the administered dose to the apical site of the gut-MPS ('oral dose') and $F_{in\,vitro}$ is the fraction of drug in the systemic circulation. In this work, $F_{in\,vitro}$ was determined based on the following equation:

$$F_{in\,vitro} = \frac{\text{AUNC}_{\text{oral}}}{D_{\text{oral}}} \Big/ \frac{\text{AUNC}_{\text{IV}}}{D_{\text{IV}}} \quad (5)$$

where $\text{AUNC}_{\text{oral}}$ refers to the area under the normalized time–concentration profile (eqn (8)) in the mixing chamber after an oral dosage of drug D_{oral} to the apical site of the gut, and similarly AUNC_{IV} corresponds to the AUNC in the mixing chamber after an IV dosage to the same with dose D_{IV}.

For the computational simulations, a unit concentration of drug was administered to the platform (1 µg ml^{-1}), which is equivalent to an administered dose of 10 µg for an apical volume of the gut MPS of 0.1 ml.

This normalization method for both the *in vivo* and *in vitro* time–concentration profiles allows direct comparison since the normalized profiles represent the response after a unit concentration in a unit distribution volume in terms of absorption and elimination rate constants (representing hepatic and renal elimination).

Table 1 Investigated drugs for module I. All drugs selected showed a renal clearance of <10%

Drug	BDDCS class	Hepatic clearance *in vitro* (ml min^{-1} kg^{-1})	Hepatic clearance *in vivo*[a] (ml min^{-1} kg^{-1})	Apparent permeability of CaCo-2 cells (10^{-6} cm s^{-1})
Training set				
Diazepam	1	6.6	15.3	36
Diclofenac	1	86.8	418	18
Fenoprofen	1	27.5	34.3	8
Ibuprofen	2	32.6	59.1	26
Lidocaine	1	15.3	82.1	44
Phenacetin	2	36.2	615	20
Propranolol	1	29.2	267	29
Warfarin	2	1.2	4.5	23
Test set				
Acetaminophen	1	2.5	6.3	37
Clozapine	2	20.8	160	31
Imipramine	1	42.8	318	7
Oxazepam	2	6.9	38.5	60
Sildenafil	1	24.4	89.8	31

[a] Intrinsic clearance values *in vivo* based on a well-stirred model from Hallifax *et al.* (2010).[56]

Table 2 Investigated drugs for module II. All drugs show both a relevant renal and hepatic clearance as well as divergent permeability

Drug	BDDCS class	Fraction excreted unchanged parent drug (%)	Apparent permeability of CaCo-2 cells (10^{-6} cm s^{-1})	Apparent permeability of MDR1-MDCK cells (10^{-6} cm s^{-1})	Hepatic clearance *in vitro* (ml min^{-1} kg^{-1})	Hepatic clearance *in vivo*[c] (ml min^{-1} kg^{-1})
Training set						
Betaxolol	1	15	12	20[a]	7.4	8.6
Linezolid	1	30	36	10[a]	2.1	1.9
Pindolol	3	54	20	60	7.8	9.6
Prednisolone	1	16	19	20[a]	30.0	27.1
Quinidine	1	19	12	AB: 2[b] BA: 7	18	34.2
Ranitidine	3	30	3	0.4	3.0	4.38
Theophylline	1	18	63	65[a]	2.6	2.6
Timolol	1	15	12	18	4.4	49.3
Test set						
Acebutolol	1	27	2	2	5.1	5.3
Alprazolam	1	20	3	AB: 37 BA: 33	2.1	2.1
Indomethacin	2	15	13	AB: 16 BA: 21	27.1	126
Ketoprofen	2	50	33	20	11.0	77.5
Nadolol	3	73	1	1	7.7	3.5

[a] Reported values are derived using CaCo-2 cells (see section 'Pharmacokinetic data' for more detail). [b] AB: apical to basal; BA: basal to apical. [c] Intrinsic clearance values *in vivo* based on a well-stirred model from Hallifax *et al.* (2010)[56] and from Paixao *et al.* (2010)[57] for linezolid.

The following design parameters were investigated (*i.e.* fitted): medium volumes for gut, liver and mixing chamber (multi-MPS platform I) or gut, liver and kidney medium volumes and the luminal flow to the kidney ($Q_{\text{kid,lum}}$, multi-MPS platform II). To reduce the number of fitting parameters in platform II, the mixing chamber volume was fixed based on the results in platform I. Standard errors for these parameters were estimated based on a Jacobian matrix[28] provided by the Matlab built-in function *lsqnonlin*.

Prior to estimation, certain limits on the range of design parameters to be fitted were imposed based on experimental feasibility and practicality. For medium volumes in each MPS and the mixing chamber the allowable range was 0.1–2 ml, and for the filtered flow to the kidney the allowable range was 1–10 ml per day. Remaining model parameters were fixed as given in Tables 3 and 4 for platforms I and II, respectively.

Direct scaling. A direct scaling approach identifies *in vitro* parameter values by linear scaling of corresponding *in vivo* parameters.

Various biological characteristics can be the focus, such as biomass or cell numbers,[11] organ blood volume or blood flow. A commonly focus is to use the *in vivo* organ volume-to-blood flow ratio[15] in the *in vitro* platform, which results in the same residence time of a compound in that organ. Hence such design strategies are based on relative sizes rather than biological functions.

To apply this approach to MPS design, the design parameter values (*i.e.*, all model parameters) were determined by scaling the corresponding *in vivo* parameters as follows:

$$p_{in\,vitro} = \frac{p_{in\,vivo}}{\text{SF}} \tag{6}$$

where $p_{in\,vitro}$ is the design parameter, $p_{in\,vivo}$ is the corresponding *in vivo* parameter and SF is a scaling factor. Using the concept of micro- and nano-humans being 10^{-6} or 10^{-9} the size of a human,[15] we designed both micro- and nano-human scale *in vitro* platforms by using the scaling factors of 10^{6} and 10^{9}, respectively. All cell numbers, organ volumes and flows

Table 3 Parameter values used for scaling in module I

Parameter	Human values (70 kg)	Direct scaling Milli-human (70 mg)	Direct scaling Micro-human (70 µg)	Allometric scaling[c] Micro-human (70 mg)	Allometric scaling[c] Nano-human (70 µg)	Multi-functional scaling
Q_{sys}[b] (ml per day)	9.4×10^{6}	9.4	9.4×10^{-3}	259	1.0	30
Q_{gut}[b] (ml per day)	$0.10 \times Q_{\text{sys}}$	$0.75 \times Q_{\text{sys}}$				
Q_{liv}[b] (ml per day)	$0.05 \times Q_{\text{sys}}$	$0.25 \times Q_{\text{sys}}$				
A_{gut}[a] (cm^2)	30×10^{4}	30×10^{-2}	30×10^{-5}	1.4×10^{-1}[d]	7.7×10^{-4}[d]	4.67
$V_{\text{gut,ap}}$[b] (ml)	510	0.5×10^{-3}	0.5×10^{-6}	4.6×10^{-3}	0.7×10^{-5}	0.1
$V_{\text{gut,bas}}$[b] (ml)	510	0.5×10^{-3}	0.5×10^{-6}	4.6×10^{-3}	0.7×10^{-5}	0.6 ± 0.03[e]
V_{liv}[b] (ml)	1800	1.8×10^{-3}	1.8×10^{-6}	3.9×10^{-3}	1.1×10^{-5}	0.3 ± 0.01[e]
V_{mix}[b] (ml)	5300	5.3×10^{-3}	5.3×10^{-6}	5.3×10^{-3}	5.3×10^{-6}	0.4 ± 0.02[e]
Hepatocytes[c] (number)	3×10^{11}	3×10^{5}	3×10^{2}	8×10^{5}	2×10^{3}	5×10^{5}

Human volumes refer to whole organ volumes and total blood volume (V_{mix}); for all scaling approaches volumes refer to MPS media volumes. References for human values: [a] Brown *et al.* (1989).[26] [b] Valentin *et al.* (2002).[73] [c] Wikswo *et al.* (2013).[19] [d] Martin *et al.* (1985).[74] [e] Estimated using multi-functional scaling.

Table 4 Parameter values used for scaling in module II

Parameter	Human values (70 kg)	Direct scaling		Allometric scaling[c]		Multi-functional scaling
		Micro-human (70 mg)	Nano-human (70 µg)	Micro-human (70 mg)	Nano-human (70 µg)	
$Q_{sys}{}^{b}$ (ml per day)	9.4×10^6	9.4	9.4×10^{-3}	259	1.0	30
$Q_{gut}{}^{b}$ (ml per day)	$0.10 \times Q_{sys}$	$0.30 \times Q_{sys}$				
$Q_{liv}{}^{b}$ (ml per day)	$0.05 \times Q_{sys}$	$0.15 \times Q_{sys}$				
$Q_{kid}{}^{b}$ (ml per day)	$0.19 \times Q_{sys}$	$0.55 \times Q_{sys}$				
$Q_{K,lum}{}^{b}$ (ml per day)	18×10^4	0.18	1.8×10^{-4}	7.8	5.4×10^{-2}	3.0 ± 0.04^{g}
$A_{gut}{}^{a}$ (cm^2)	30×10^4	30×10^{-2}	30×10^{-5}	1.4×10^{-1f}	7.7×10^{-4f}	4.67
$A_{kid}{}^{d}$ (cm^2)	6.1×10^4	6.1×10^{-2}	6.1×10^{-6}	11.6^{e}	0.16^{e}	4.67
$V_{gut,ap}{}^{b}$ (ml)	510	0.5×10^{-3}	0.5×10^{-6}	4.6×10^{-3}	0.7×10^{-5}	0.1
$V_{gut,bas}{}^{b}$ (ml)	510	0.5×10^{-3}	0.5×10^{-6}	4.6×10^{-3}	0.7×10^{-5}	0.3 ± 0.02^{g}
$V_{liv}{}^{b}$ (ml)	1800	1.8×10^{-3}	1.8×10^{-6}	3.9×10^{-3}	1.1×10^{-5}	0.2 ± 0.03^{g}
$V_{mix}{}^{b}$ (ml)	5300	5.3×10^{-3}	5.3×10^{-6}	5.3×10^{-3}	5.3×10^{-6}	0.4
$V_{kid,ap}{}^{b}$ (ml)	155	1.6×10^{-4}	1.6×10^{-7}	1.1×10^{-3}	3.1×10^{-6}	0.1
$V_{kid,bas}{}^{b}$ (ml)	155	1.6×10^{-4}	1.6×10^{-7}	1.1×10^{-3}	3.1×10^{-6}	0.8 ± 0.3^{g}
Waste (ml)	$Q_{K,lum} \times t$					
Hepatocytes[c] (number)	3×10^{11}	3×10^5	3×10^2	8×10^5	2×10^3	5×10^5

Human volumes refer to whole organ volumes and total blood volume (V_{mix}); for all scaling approaches volumes refer to MPS media volumes. References for human values: [a] Brown *et al.* (1989).[26] [b] Valentin *et al.* (2002).[73] [c] Wikswo *et al.* (2013).[19] [d] Scotcher *et al.* (2016).[61] [e] Scaled using number of nephrons. [f] Martin *et al.* (1985).[74] [g] Estimated using multi-functional scaling.

were scaled this way. Using the resulting parameterized platform models, *in vitro* time–concentration profiles were calculated using the mechanistic models for platforms I and II. For comparison to *in vivo* concentration profiles, the *in vitro* time–concentration profiles were normalized according to eqn (4). Total media volume for the platforms was calculated based on the individual MPS volumes and the administered dose to the apical site of the gut was calculated from an initial concentration of $c_0 = 1$ µg ml^{-1}. Normalization was applied to the resulting *in vitro* time–concentration profiles as was described for the multi-functional approach.

Allometric scaling. Allometric scaling is the most common approach in MPS design due to availability of data and its accepted usage to extrapolate animal data to clinical outcome.[15,19]

For the micro- and nano-human, the required design parameters were calculated (Tables 3 and 4) according to the following equation:

$$Y = a \times M^{b} \tag{7}$$

where a and b are allometric scaling coefficients, M is bodyweight in kg and Y is the parameter of interest to be scaled.[2,19] Similar to the direct scaling approach, each parameter for each MPS in a multi-MPS platform is scaled independently. The same steps for scaling parameters and simulating time–concentration profiles were used as described for direct scaling. Normalization was applied to the resulting *in vitro* time–concentration profiles as was used for the multi-functional scaling approach.

Quantitative evaluation of exposure times

To quantitatively evaluate the performance of all three scaling approaches to produce clinically relevant exposure times, the area under the normalized time–concentration curve (AUNC) was calculated from the time of administration ($t = 0$) to the last measurement point (t_f) of the drug specific time–concentration profile by integration:

$$\text{AUNC} = \int_0^{t_f} c(t)\mathrm{d}t \tag{8}$$

The AUNC value indicates a normalized exposure duration after administration of a unit dose to a unit distribution volume, assuming complete bioavailability.

Additionally, for multi-MPS platform II, the model outcome of fraction unchanged excreted parent drug was estimated and compared to the reported clinical values for each drug.

Using the multi-functional scaling approach, the distribution of five additional drugs was simulated for each platform (Tables 1 and 2, test set) to validate the estimated design parameters. Subsequently, AUNCs were determined to evaluate the estimated design parameter values and model performance for this test set of drugs that had not been included in the design process.

Pharmacokinetic data

Drugs in the training set for multi-MPS platform I were selected based on intrinsic *in vitro* clearance values covering a wide range (1.2–86.6 ml min^{-1} kg^{-1}). Similarly, for multi-MPS platform II, including drugs with a wide range of clearance by the liver (2.1–30.0 ml min^{-1} kg^{-1}) as well as the fraction excreted unchanged drug (0.15–0.54) guided selection of the drugs. Drugs in the test set were chosen to fall within the training ranges of clearance and excreted fraction.

The training set of eight drugs for multi-MPS platform I included: diazepam,[29] diclofenac,[30] fenoprofen,[31] ibuprofen,[32] lidocaine,[33] phenacetin,[34] propranolol,[35] warfarin.[36] For multi-MPS platform II they were: betaxolol,[37] linezolid,[38] pindolol,[39] prednisolone,[40] quinidine,[41] ranitidine,[42] theophylline[43] and timolol.[44]

The test set of five drugs used in the multi-functional scaling approach to evaluate the resulting design parameters for multi-MPS platform I included: acetaminophen,[45] clozapine,[46]

imipramine,[47] oxazepam[48] and sildenafil;[49] for multi-MPS platform II: acebutolol,[50] alprazolam,[51] indomethacin,[52] ketoprofen[53] and nadolol.[54] References indicate source of time–concentration profiles and administered dose. Volumes of distribution and oral bioavailability were derived from literature.[55] Data were digitized in graphical format (Plot Digitizer v2.6.8, https://sourceforge.net/projects/plotdigitizer/). More detailed information of the investigated drugs for both platforms is presented in Tables 1 and 2.

Intrinsic *in vitro* clearance values by hepatocytes for all drugs were taken from ref. 56, except for linezolid.[57] Clearance values reported (in ml min^{-1} kg^{-1} bodyweight) were scaled to a reference human with a bodyweight of 70 kg (ref. 26) and normalized to a hepatocyte count of 3×10^{11} (clearance/hepatocyte; Tables 1 and 2).[19] Subsequently, this value was scaled linearly to clearance in the liver MPS using 5×10^5 hepatocytes.

Permeability values for CaCo-2 cells were taken from ref. 58, except for fenoprofen,[59] phenacetin,[60] and linezolid and prednisolone.[61] Permeability values of MDR1-MDCK cells for pindolol and timolol were derived from ref. 62 and for quinidine from ref. 63. For betaxolol, linezolid, prednisolone and theophylline corresponding CaCo-2 cell permeability values were used[61] (recent work indicates that there is a linear relationship between estimated permeability values from CaCo-2 and MDR1-MDCK cells[64–66]). Fraction excreted unchanged drug as well as drug classes were derived from ref. 67.

3. Results and discussion

The aim of this work was to develop a function-based scaling methodology for designing multi-MPS platforms. This methodology bases design on multiple MPS functions simultaneously and explicitly considers the application of interest, *e.g.*, pharmacokinetics or other pharmacological applications of small molecule drugs.

The devised multi-functional scaling approach specifies an objective that represents the desired pharmacological or biological mechanisms the integrated multi-MPS platform should reproduce, and estimates parameter values for platform design and operation that best satisfy the objective function.

This novel approach was tested with two platforms relevant to the study and prediction of drug exposure. Multi-MPS platform I, including gut and liver MPSs, provides a biological representation of absorption through gut epithelium, metabolism by the liver, and distribution between these and a non-biological mixing chamber that approximates the collection of blood by venous circulation before it is recirculated by the heart in human. Multi-MPS platform II adds a kidney MPS to include additional elimination of a drug, which is a critical modulator of drug exposure and PK for numerous compounds. Active development and testing of gut, liver and kidney MPSs related to those described in this study's models are underway in several laboratories,[11,12] so while the study is theoretical, its applicability to actual MPS technologies is relevant today.

Multi-functional scaling

For both platforms I and II, the model output for time–concentration profiles based on design parameters (Tables 3 and 4) identified

by the optimization algorithm agrees well with reported clinical data (Fig. 2) for a majority of the drugs, although not all were equally well captured. In platform I, the model description for diazepam captured the elimination phase while the observed maximum concentration is about 2-fold less. The description for lidocaine was systematically off. Warfarin showed a 2.5-fold higher concentration than the reported data, but a similar decline after the end of the absorption phase can be seen. These are possibly due to differences between *in vitro* and *in vivo* clearance values of these drugs by hepatocytes (Table 1). In platform II, the model profile for ranitidine showed a 3-fold higher maximum concentration compared to the clinical data, but a similar elimination phase. For quinidine, the clearance from the system appears to be faster than reported *in vivo*, suggesting differences between *in vitro* and *in vivo* hepatic clearance values.

Quantitative evaluation of these drug profiles was performed by assessing area under the normalized time–concentration curve for both platforms. Clinically observed drug exposures were well recapitulated in the theoretical *in vitro* platforms. On average, the ratio of *in vivo* to *in vitro* drug exposures was (mean and standard deviation): 0.7 ± 0.3 and 1.0 ± 0.6 for platforms I and II, respectively (Fig. 3). Various methods are presently used for *in vitro–in vivo* extrapolation of PK, where human PK characteristics are extrapolated from measurements made in animals, hepatocyte cultures or hepatocyte microsomes. It is informative to compare those to the results of our theoretical gut–liver and gut–liver–kidney MPS platforms designed using multi-functional scaling. A common measure of acceptance is whether extrapolated values are within $2\times$ or $3\times$ of the (eventually) measured *in vivo* human PK parameter value.[56,68–70] By that measure, results from our platforms I and II designed by multi-functional scaling easily fall within the accepted extrapolative capabilities of these other approaches, showing promise for using our multi-functional MPS design approach for pharmacokinetic/pharmacodynamic (PK/PD) applications.

Fraction excreted parent drug from the system in platform II was on average (3.0 ± 1.4)-fold higher than found *in vivo* (range: 15–54%; Table 2 and Fig. S1, ESI†). Possibly, permeability through the MDR1-MDCK-monolayer is considerably lower *in vitro* resulting in less reabsorption of the parent drug than observed *in vivo*. This in turn leads to an increased excreted amount of drug, which is then not available for hepatic clearance.

Estimated design parameter values are reported in Tables 3 and 4. In platform I, the combination of simulated hepatocyte number (5×10^5), the surface area of the gut MPS (4.67 cm^2) and the resulting total media volume on the order of milliliters is likely to supply sufficient nutrients, *e.g.* oxygen and glucose, to the cell cultures based upon standard laboratory cell culture protocols. Introducing boundaries (lower and upper limit) for medium volumes allowed the multi-functional scaling approach to identify an optimal combination of design parameter values to satisfy the specific study purpose as well as these practical constraints. This is in contrast to direct scaling and allometric scaling approaches, in which the scaling is applied without considering the application of interest and interaction between MPSs.
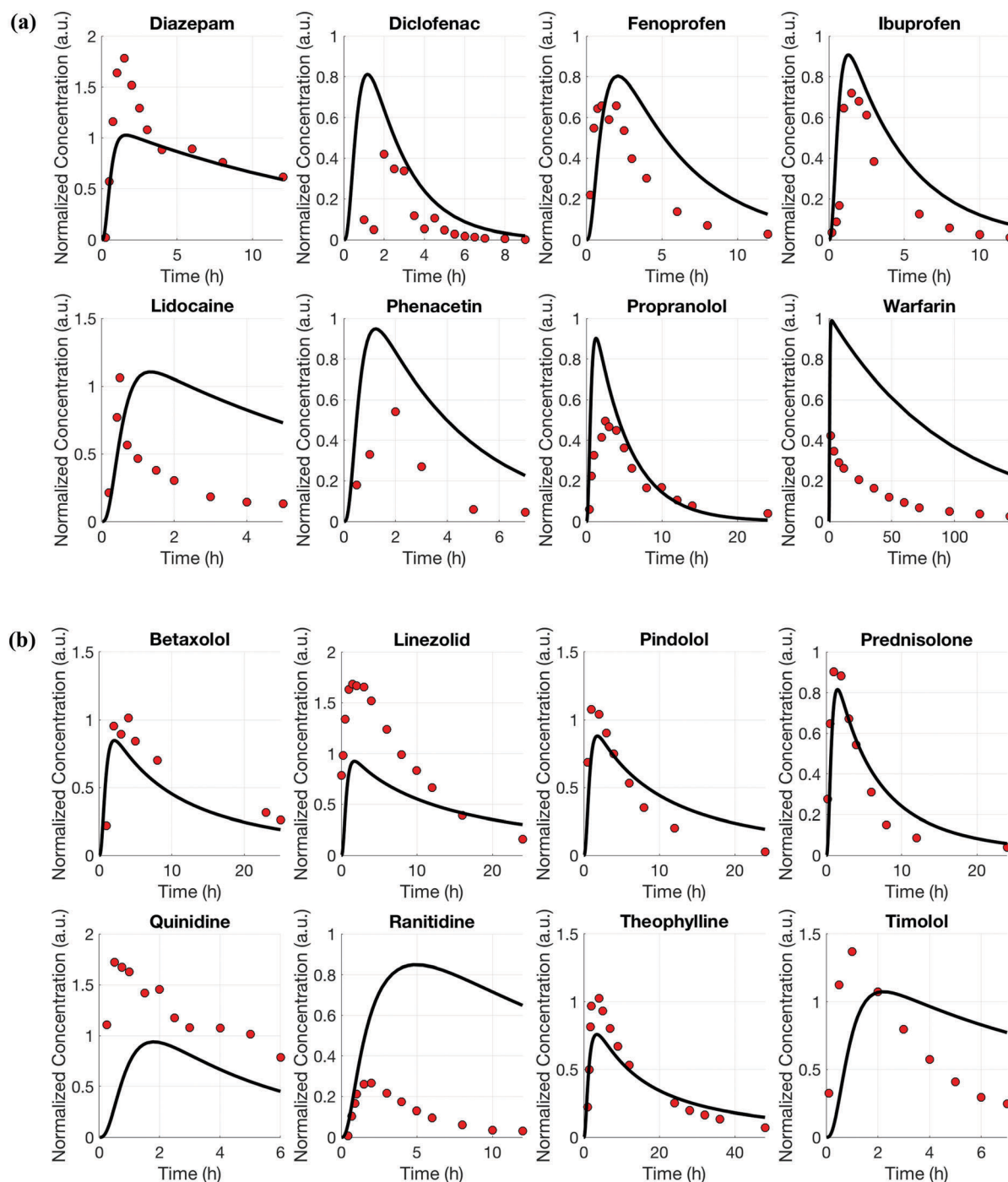
Fig. 2 Model based description (black lines) for drug distribution in platform I (a) and platform II (b) after application of the multi-functional scaling approach. Reported clinical data (red dots) of eight drugs that are mainly cleared by the liver (a) or by the liver and the kidney (b) were simultaneously investigated to inform one platform design.

Similarly, in platform II, the total media volume is in the order of milliliters, the same number of hepatocytes were simulated and surface areas for kidney and gut MPSs are in accordance with commonly used transwells and inserts (Table 4). Moreover, the semi-closed architecture of this platform allows a continuous medium supply and required nutrients.

Using the test set of five drugs, quantitative evaluation of the profiles (Fig. 4) showed on average a (1.3 ± 0.8)-fold higher and

(0.7 ± 0.5)-fold lower drug exposure than *in vivo* for multi-MPS platforms I and II, respectively (Fig. 5).

Direct and allometric scaling

The design of multi-MPS platforms I and II was also performed using direct and allometric scaling. Feasibility of each of these scaling approaches was assessed by estimating drug exposures for the same training set (eight drugs per platform) and
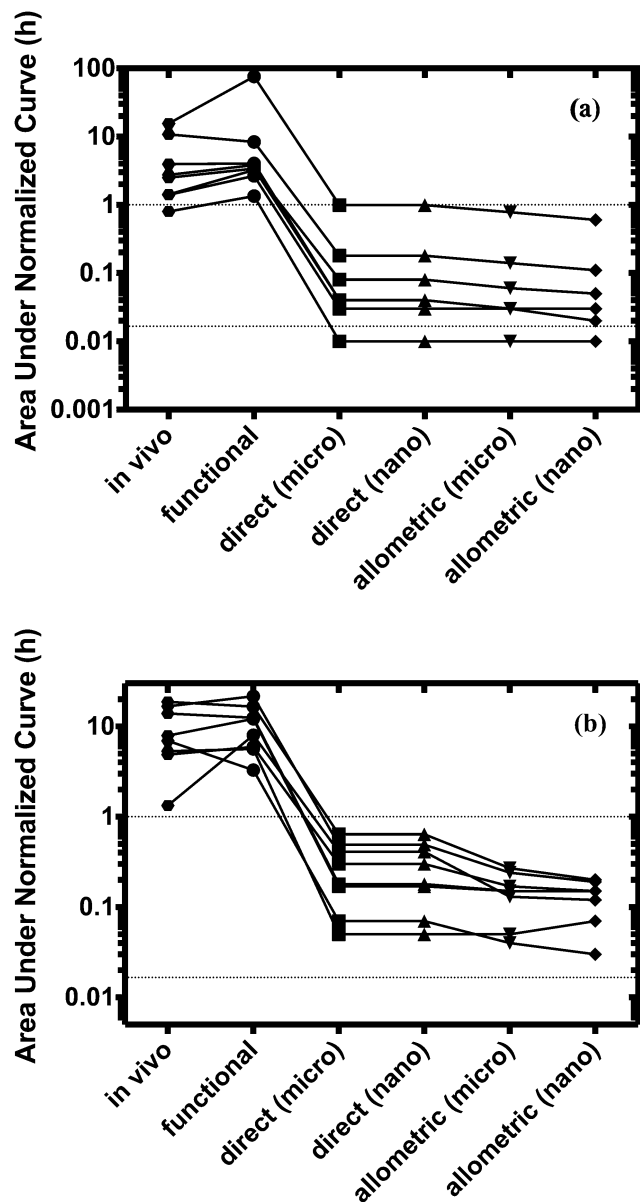
Fig. 3 Estimated normalized exposure (h) from the clinical data (*in vivo*) and from all three scaling approaches (functional, direct and allometric) for (a) platform I and (b) platform II. Upper and lower dotted horizontal lines indicate 1 h and 1 min, respectively. Using the multi-functional scaling approach, a design for both platforms was established yielding exposure times close to *in vivo* values (hours). In contrast, both direct and allometric scaling resulted in exposure times of minutes to seconds.

and would require more frequent medium changes. However, choosing a different scaling factor or estimating these parameters based on a milli-human (70 g), would increase the absolute parameter values, but not changing the estimation of the area under the normalized curve (due to linear kinetics).

The model profiles underpredicted the actual human plasma drug time–concentration profiles for all drugs as can be seen in Fig. 3.

Direct scaling in platform I was able to capture the concentration maximum. However, both platforms and approaches showed extremely fast clearance (within minutes) compared to *in vivo* (Fig. S2, ESI†). On average, 50–300-fold lower drug exposure times were estimated for both platforms.

Three major differences in the multi-functional scaling approach compared to direct or allometric scaling are as follows: (1) this approach optimizes a design by accounting for multiple biological functions of each MPS simultaneously, (2) it works to optimize the design for multiple MPSs simultaneously rather than independently, and (3) it explicitly accounts for planned research applications of a (multi-)MPS platform during design. In comparison, direct and allometric scaling approaches focus on reproducing single characteristics independently of one another, and these are typically size-related (mass, volume, area, *etc.*). As demonstrated in the comparisons made among approaches, the multi-functional scaling approach provided a better representation of *in vivo* drug exposure than did either of the others. Points 1 and 2 are clearly desirable to best inform designs that represent simultaneously all functions related to all MPS. The critical importance of point 3 becomes evident when looking at the design parameter values: the multi-functional scaling resulted in medium volumes substantially larger than the other two methods because this was required to recapitulate *in vivo* drug exposures in the multi-MPS platforms studied. This demonstrates that hewing closely to *in vivo* tissue characteristics, while intuitively appealing, will not automatically result in MPS designs that reproduce desired functions – direct and allometric scaling failed to recapitulate the relevant pharmacology properties, in this case drug exposures.

A thought experiment further demonstrates that different planned applications may require different MPS designs. If the desire had been to reproduce concentration profiles for cell-produced mediators such as cytokines or growth factors, then using the multi-functional scaling algorithm might result in much smaller volume-to-tissue ratios for design parameters than it did for drug exposure. This is because the volumes would need to be small (comparable to extracellular volumes *in vivo*) to result in mediator concentrations similar to *in vivo* for a given cell number within an MPS, whereas larger volumes would cause excess dilution.

Normalized exposure times were calculated and used to quantitatively evaluate the performance of all the scaling approaches. Only the multi-functional scaling methodology captured exposure times similar to *in vivo*, whereas direct and allometric scaling resulted in exposure times that were orders of magnitude smaller.

Based on our experience culturing these cells, the operation of MPS scaled with the latter approaches will be severely limited
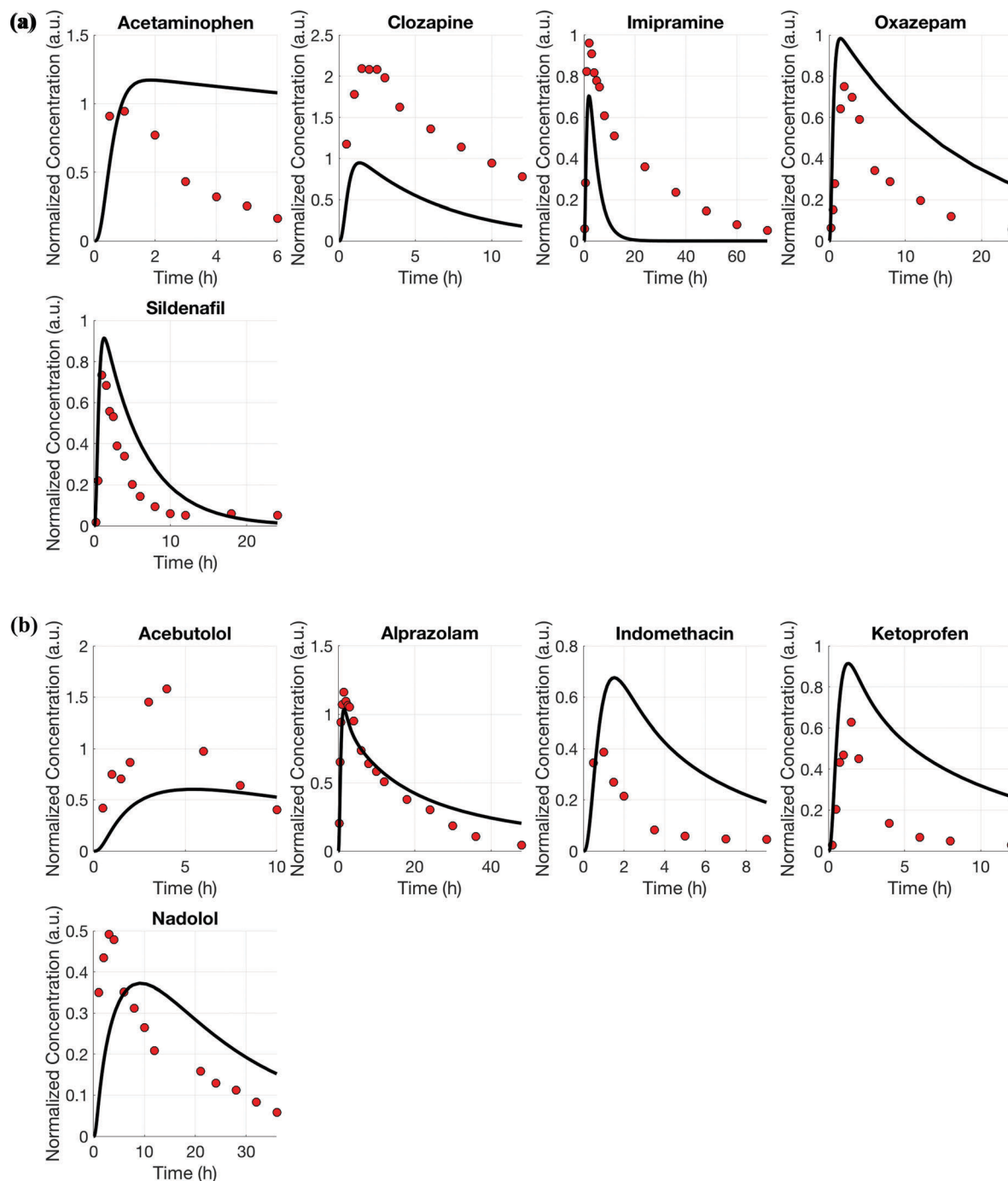
subsequent comparison to *in vivo* results. The estimated design parameters were also compared to those from the multi-functional scaling approach. The test set of five drugs was not evaluated using direct and allometric scaling.

Scaling of the relevant model parameters for multi-MPS platforms I and II to simulate a theoretical micro-human (70 mg) or nano-human (70 µg, Tables 3 and 4) lead to highly impractical design parameter values. Due to the relative high number of cells and small medium volumes, these systems would most likely be nutrient limited (*e.g.* oxygen or glucose)

Fig. 4 Model-based prediction for five drug distributions in vitro for (a) multi-MPS platform I and (b) multi-MPS platform II using the estimated design parameters from the multi-functional scaling approach. In general, the predictions are acceptable.

by nutrient depletion due to the small medium-to-tissue ratios in closed- and semi-closed loop platforms described. Alternatives to alleviate these limitations would be to change medium much more frequently than is typical for closed-loop systems (every 2–3 days) or go to continuous fresh medium feed in an open-loop system. These are valid operational approaches, but bring different limitations by limiting exposure time to drug and thereby drug metabolism, as well as frequently or continuously removing cell-produced mediators that might be of interest for study of MPS–MPS interactions.

An obvious challenge in utilizing this new multi-functional scaling approach is the need for appropriate data (both in vitro and in vivo) to inform the objective function as well as to parameterize the necessary system models. The demonstration cases herein, focused on pharmacokinetics, benefited from the large body of available data on in vivo drug pharmacokinetics and in vitro cell biological data.

Although this work primarily focused on the drug profiles in the plasma, a potential improvement would be to include drug
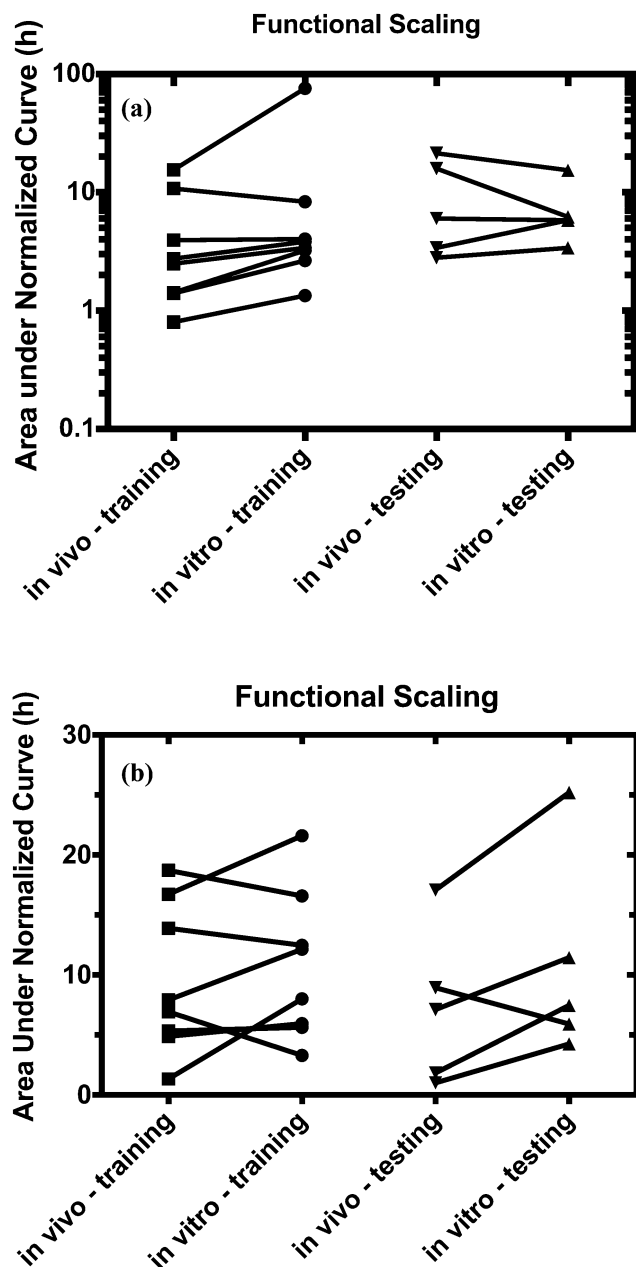
Fig. 5 Comparison of estimated normalized exposure times from *in vivo* (clinical data) and the *in vitro* platform using design parameter values determined by the multi-functional scaling approach for both (a) platform I and (b) platforms II. Overall, both multi-MPS platforms yield exposure times very similar to the *in vivo* values. Using this platform as a predictive tool, the resulting exposure times are also in close proximity to the actual values for both platforms.

concentrations in each organ of interest in the objective function along with plasma drug profiles. This would help the final designed multi-MPS platforms achieve pharmacologically relevant drug concentrations in each MPS and better enable studying drug interactions with uptake transporters or metabolizing enzymes as well as pharmacodynamic effects. However, a limitation to doing so would be the availability of data at the organ level.

Improving the cell to media ratio will also likely affect the volume of distribution. For instance, the multi-functional scaling resulted in considerably smaller media volumes for both multi-MPS platforms I and II than those currently used in typical transwell-based MPSs.[13] The reduction in volume-to-tissue ratio will affect cellular uptake rates and, hence, drug clearance. For larger media volumes (compared to the cell volumes), this effect may become negligible and would therefore lead to a non-physiological response, which will subsequently affect the translation to *in vivo*. Recent work demonstrated the need for improved cell to media ratios: secreted factors by dendritic cells stimulated CD4+ primary human T cells only, when a physiologically relevant cell to media volume ratio was provided[22] (media volumes ∼ microliters). On the contrary, smaller media volumes for commonly used cell cultures may be detrimental as limited nutrients are provided.

Accurate recapitulation of physiological processes is essential for a successful translation to clinical outcomes. The investigated theoretical kidney MPS covers the functions of reabsorption, secretion, filtration and excretion. In the modeled kidney MPS, the filtration and excretion processes are dictated by hardware (*i.e.* practical constraints), whereas reabsorption, and secretion occur through proximal tubular epithelial tissue. This may lead to a systematically different concentration gradient between the lumen and interstitial space of the kidney MPS resulting in an over-prediction of excreted unchanged drug. Mimicking the 3D microarchitecture of the human kidneys *in vitro* would potentially improve the description of filtration and excretion.

It is likely that the larger the set of relevant functional considerations included when applying the multi-functional scaling methodology described herein, the better the resulting platform design. For example, the case studies herein focused on recapitulating clinically relevant drug exposures may be further improved with the inclusion of additional *a priori* knowledge about physicochemical properties of drugs (molecular weight, charge, lipophilicity), the volume of distribution, bioavailability and the fraction of unbound drug. Similarly, inclusion of donor-to-donor variability for the simulated liver or kidney MPSs could be considered in the multi-functional scaling methodology for multi-MPS platforms. Moreover, a larger set of drugs and drugs with different classifications (BDDCS[67]) could be used as training and test sets to further verify the methodology's applicability. Additionally, multi-MPS platforms could be used to study time–concentration profiles of metabolites and metabolite formation, since these can be important for both efficacy and adverse effects,[71] depending on the drug.

Considering the biology of MPSs, data obtained from more advanced MPS technologies will also further improve multi-MPS design strategies. For example, metabolism by the gut contributes considerably to PK *in vivo* and bioavailability of drugs. Therefore, the use of human primary cells instead of cell lines are likely to further improve the predictability of such systems.

While our case studies have necessarily used data from existing drugs, the desire to design MPS platforms to predict exposure for new investigational entities raises the question of which platform to use in the absence of clinical data. A decision

can be based on physicochemical properties to assess if the compound would be mainly metabolized by the liver or excreted *via* kidneys.[72]

The methodology described herein can be applied and readily adapted to other study objectives such as normal and disease biology, pharmacodynamics, toxicity or optimization of media compositions. For instance, studying diabetes would require a carefully designed multi-MPS platform to recapitulate relevant glucose and glucose-induced insulin levels. Potentially, a fat–muscle–liver–pancreas–gut platform would serve this purpose and chronic exposures of increased glucose levels and the effect on insulin production by the pancreas MPS may be more adequately investigated.

While MPSs are a promising technology for improving translation of preclinical results to clinical outcomes, the promise will be limited if the design is not able to capture the essence of *in vivo* physiology appropriately to enable *in vitro–in vivo* translation. Thus, the multi-functional scaling approach presents a novel framework to tailor integrated multi-MPS platforms to a specific and intended study objective across multiple areas of interest.

4. Conclusion

The novel multi-functional scaling approach described here allowed the design of integrated multi-MPS platforms for relevant pharmacological applications. In the applications demonstrated here, the resulting design parameter values are practical and can be easily implemented. The approach can be readily adapted to various multi-MPS platforms for a variety of study purposes. Current scaling approaches (direct and allometric scaling) were not able to meet the study objective in this work. Recapitulation of *in vivo* drug exposure times *in vitro* allows to establish exposure–response relationships and thus for more relevant studies of pharmacodynamics and toxicity.

Acknowledgements

References

1 H. E. Abaci and M. L. Shuler, *Integr. Biol.*, 2015, **7**, 383–391.
2 C. Moraes, J. M. Labuz, B. M. Leung, M. Inoue, T. H. Chun and S. Takayama, *Integr. Biol.*, 2013, **5**, 1149–1161.
3 U. Marx, T. B. Andersson, A. Bahinski, M. Beilmann, S. Beken, F. R. Cassee, M. Cirit, M. Daneshian, S. Fitzpatrick, O. Frey, C. Gaertner, C. Giese, L. Griffith, T. Hartung, M. B. Heringa, J. Hoeng, W. H. de Jong, H. Kojima, J. Kuehnl, M. Leist, A. Luch, I. Maschmeyer, D. Sakharov, A. J. Sips, T. Steger-Hartmann, D. A. Tagle, A. Tonevitsky, T. Tralau, S. Tsyb, A. van de Stolpe,

R. Vandebriel, P. Vulto, J. Wang, J. Wiest, M. Rodenburg and A. Roth, *ALTEX*, 2016, **33**, 272–321.
4 S. Y. Chang, E. J. Weber, K. P. Van Ness, D. L. Eaton and E. J. Kelly, *Clin. Pharmacol. Ther.*, 2016, **100**, 464–478.
5 D. D. Huh, *Ann. Am. Thorac. Soc.*, 2015, **12**(suppl 1), S42–S44.
6 B. Atac, I. Wagner, R. Horland, R. Lauster, U. Marx, A. G. Tonevitsky, R. P. Azar and G. Lindner, *Lab Chip*, 2013, **13**, 3555–3561.
7 A. Grosberg, A. P. Nesmith, J. A. Goss, M. D. Brigham, M. L. McCain and K. K. Parker, *J. Pharmacol. Toxicol. Methods*, 2012, **65**, 126–135.
8 M. M. Laronda, J. E. Burdette, J. J. Kim and T. K. Woodruff, *Stem Cell Res. Ther.*, 2013, **4**, 1–5.
9 A. Marsano, C. Conficconi, M. Lemme, P. Occhetta, E. Gaudiello, E. Votta, G. Cerino, A. Redaelli and M. Rasponi, *Lab Chip*, 2016, **16**, 599–610.
10 K. Domansky, W. Inman, J. Serdy, A. Dash, M. H. Lim and L. G. Griffith, *Lab Chip*, 2010, **10**, 51–58.
11 I. Maschmeyer, A. K. Lorenz, K. Schimek, T. Hasenberg, A. P. Ramme, J. Hubner, M. Lindner, C. Drewell, S. Bauer, A. Thomas, N. S. Sambo, F. Sonntag, R. Lauster and U. Marx, *Lab Chip*, 2015, **15**, 2688–2699.
12 C. Oleaga, C. Bernabini, A. S. Smith, B. Srinivasan, M. Jackson, W. McLamb, V. Platt, R. Bridges, Y. Cai, N. Santhanam, B. Berry, S. Najjar, N. Akanda, X. Guo, C. Martin, G. Ekman, M. B. Esch, J. Langer, G. Ouedraogo, J. Cotovio, L. Breton, M. L. Shuler and J. J. Hickman, *Sci. Rep.*, 2016, **6**, 20030.
13 J. Yu, N. A. Cilfone, E. M. Large, U. Sarkar, J. S. Wishnok, S. R. Tannenbaum, D. J. Hughes, D. A. Lauffenburger, L. G. Griffith, C. L. Stokes and M. Cirit, *CPT: Pharmacometrics Syst. Pharmacol.*, 2015, **4**, 585–594.
14 Z. Xu, E. Li, Z. Guo, R. Yu, H. Hao, Y. Xu, Z. Sun, X. Li, J. Lyu and Q. Wang, *ACS Appl. Mater. Interfaces*, 2016, **8**, 25840–25847.
15 J. H. Sung, C. Kam and M. L. Shuler, *Lab Chip*, 2010, **10**, 446–455.
16 E. W. Esch, A. Bahinski and D. Huh, *Nat. Rev. Drug Discovery*, 2015, **14**, 248–260.
17 E. L. LeCluyse, R. P. Witek, M. E. Andersen and M. J. Powers, *Crit. Rev. Toxicol.*, 2012, **42**, 501–548.
18 R. Baudoin, J. M. Prot, G. Nicolas, J. Brocheton, C. Brochot, C. Laegallais, H. Benech and E. Leclerc, *Xenobiotica*, 2013, **43**, 140–152.
19 J. P. Wikswo, E. L. Curtis, Z. E. Eagleton, B. C. Evans, A. Kole, L. H. Hofmeister and W. J. Matloff, *Lab Chip*, 2013, **13**, 3496–3511.
20 N. Ucciferri, T. Sbrana and A. Ahluwalia, *Front. Bioeng. Biotechnol.*, 2014, **2**, 74.
21 C. L. Stokes, M. Cirit and D. A. Lauffenburger, *CPT: Pharmacometrics Syst. Pharmacol.*, 2015, **4**, 559–562.
22 J. P. Wikswo, *Exp. Biol. Med.*, 2014, **239**, 1061–1072.
23 L. Vernetti, A. Gough, N. Baetz, S. Blutt, J. R. Broughman, J. A. Brown, J. Foulke-Abel, N. Hasan, J. In, E. Kelly, O. Kovbasnjuk, J. Repper, N. Senutovitch, J. Stabb, C. Yeung, N. C. Zachos, M. Donowitz, M. Estes,

J. Himmelfarb, G. Truskey, J. P. Wikswo and D. L. Taylor, *Sci. Rep.*, 2017, **7**, 42296.

24 V. Sharma and J. H. McNeill, *Br. J. Pharmacol.*, 2009, **157**, 907–921.

25 R. V. Overgaard, S. H. Ingwersen and C. W. Tornoe, *CPT: Pharmacometrics Syst. Pharmacol.*, 2015, **4**, 565–575.

26 R. P. Brown, M. D. Delp, S. L. Lindstedt, L. R. Rhomberg and R. P. Beliles, *Toxicol. Ind. Health*, 1997, **13**, 407–484.

27 ICRP, *Ann. ICRP*, 2002, **32**, 5–265.

28 P. H. Richter, *TDA Prog. Rep.*, 1995, **42**, 107–137.

29 H. Friedman, D. J. Greenblatt, G. R. Peters, C. M. Metzler, M. D. Charlton, J. S. Harmatz, E. J. Antal, E. C. Sanborn and S. F. Francom, *Clin. Pharmacol. Ther.*, 1992, **52**, 139–150.

30 J. V. Willis, M. J. Kendall, R. M. Flinn, D. P. Thornhill and P. G. Welling, *Eur. J. Clin. Pharmacol.*, 1979, **16**, 405–410.

31 J. F. Nash, L. D. Bechtol, R. J. Bopp, K. Z. Farid, C. T. Spradlin and C. A. Bunde, *J. Pharm. Sci.*, 1979, **68**, 1087–1090.

32 D. R. Abernethy and D. J. Greenblatt, *Arthritis Rheum.*, 1985, **28**, 1117–1121.

33 P. N. Bennett, L. J. Aarons, M. R. Bending, J. A. Steiner and M. Rowland, *J. Pharmacokinet. Biopharm.*, 1982, **10**, 265–281.

34 Z. Q. Qu, X. D. Li, H. L. Liu, P. He, X. Zhang and M. C. Wu, *Int. J. Clin. Pharmacol. Ther.*, 2007, **45**, 55–62.

35 L. Borgstroem, C. Johansson, H. Larsson and R. Lenander, *J. Pharmacokinet. Biopharm.*, 1981, **9**, 419–429.

36 J. Dingemanse and P. Hoever, *Drugs R&D*, 2013, **13**, 145–151.

37 J. F. Giudicelli, M. Chauvin, C. Thuillez, C. Richer, G. Bianchetti, R. Gomeni and P. L. Morselli, *Br. J. Clin. Pharmacol.*, 1980, **10**, 41–49.

38 M. S. Dryden, *J. Antimicrob. Chemother.*, 2011, **66**(suppl 4), iv7–iv15.

39 R. Gugler, W. Herold and H. J. Dengler, *Eur. J. Clin. Pharmacol.*, 1974, **7**, 17–24.

40 M. E. Pickup, *Clin. Pharmacokinet.*, 1979, **4**, 111–128.

41 R. A. Wooding-Scott, J. Smalley, J. Visco and R. L. Slaughter, *Br. J. Clin. Pharmacol.*, 1988, **26**, 415–421.

42 M. L. McFayden, P. I. Folb, R. Miller, I. N. Marks and M. G. Moshal, *Eur. J. Clin. Pharmacol.*, 1983, **24**, 441–447.

43 V. Rovei, F. Chanoine and M. Strolin Benedetti, *Br. J. Clin. Pharmacol.*, 1982, **14**, 769–778.

44 A. Bobik, G. L. Jennings, P. Ashley and P. I. Korner, *Eur. J. Clin. Pharmacol.*, 1979, **16**, 243–249.

45 M. D. Rawlins, D. B. Henderson and A. R. Hijab, *Eur. J. Clin. Pharmacol.*, 1977, **11**, 283–286.

46 W. Tassaneeyakul, K. Kittiwattanagul, S. Vannaprasaht, J. Kampan, A. Tawalee, P. Puapairoj, S. Tiamkao, S. Juthagridsada, V. Kukongviriyapan and W. Tassaneeyakul, *J. Pharm. Pharm. Sci.*, 2005, **8**, 47–53.

47 D. A. Ciraulo, J. G. Barnhill and J. H. Jaffe, *Clin. Pharmacol. Ther.*, 1988, **43**, 509–518.

48 J. Sonne, S. Loft, M. Døssing, A. Vollmer-Larsen, K. L. Olesen, M. Victor, F. Andreasen and P. B. Andreasen, *Eur. J. Clin. Pharmacol.*, 1988, **35**, 385–389.

49 D. J. Nichols, G. J. Muirhead and J. A. Harness, *Br. J. Clin. Pharmacol.*, 2002, **53**, 5S–12S.

50 C. M. Kaye, C. R. Kumana, M. Leighton, J. Hamer and P. Turner, *Clin. Pharmacol. Ther.*, 1976, **19**, 416–420.

51 D. J. Greenblatt and C. E. Wright, *Clin. Pharmacokinet.*, 1993, **24**, 453–471.

52 H. W. Emori, G. D. Champion, R. Bluestone and H. E. Paulus, *Ann. Rheum. Dis.*, 1973, **32**, 433.

53 F. Jamali and D. R. Brocks, *Clin. Pharmacokinet.*, 1990, **19**, 197–217.

54 M. Korting-Schäfer, N. Bach, H. Knauf and E. Mutschler, *Eur. J. Clin. Pharmacol.*, 1984, **26**, 125–127.

55 M. V. Varma, R. S. Obach, C. Rotter, H. R. Miller, G. Chang, S. J. Steyn, A. El-Kattan and M. D. Troutman, *J. Med. Chem.*, 2010, **53**, 1098–1108.

56 D. Hallifax, J. A. Foster and J. B. Houston, *Pharm. Res.*, 2010, **27**, 2150–2161.

57 P. Paixao, L. F. Gouveia and J. A. Morais, *Eur. J. Pharm. Sci.*, 2010, **39**, 310–321.

58 P. Paixao, L. F. Gouveia and J. A. Morais, *Eur. J. Pharm. Sci.*, 2010, **41**, 107–117.

59 R. Gozalbes, M. Jacewicz, R. Annand, K. Tsaioun and A. Pineda-Lucena, *Bioorg. Med. Chem.*, 2011, **19**, 2615–2624.

60 S. Khan, H. Batchelor, P. Hanson, Y. Perrie and A. R. Mohammed, *J. Pharm. Sci.*, 2011, **100**, 4281–4294.

61 D. Scotcher, C. Jones, A. Rostami-Hodjegan and A. Galetin, *Eur. J. Pharm. Sci.*, 2016, **94**, 59–71.

62 J. D. Irvine, L. Takahashi, K. Lockhart, J. Cheong, J. W. Tolan, H. E. Selick and J. R. Grove, *J. Pharm. Sci.*, 1999, **88**, 28–33.

63 M. Patel, N. K. Mandava, D. Pal and A. K. Mitra, *Int. J. Pharm.*, 2014, **464**, 196–204.

64 X. Jin, T. L. Luong, N. Reese, H. Gaona, V. Collazo-Velez, C. Vuong, B. Potter, J. C. Sousa, R. Olmeda, Q. Li, L. Xie, J. Zhang, P. Zhang, G. Reichard, V. Melendez, S. R. Marcsisin and B. S. Pybus, *J. Pharmacol. Toxicol. Methods*, 2014, **70**, 188–194.

65 A. Avdeef and K. Y. Tam, *J. Med. Chem.*, 2010, **53**, 3566–3584.

66 A. Braun, S. Hämmerle, K. Suda, B. Rothen-Rutishauser, M. Günthert, S. D. Krämer and H. Wunderli-Allenspach, *Eur. J. Pharm. Sci.*, 2000, **11**, S51–S60.

67 L. Z. Benet, F. Broccatelli and T. I. Oprea, *AAPS J.*, 2011, **13**, 519–547.

68 G. W. Caldwell, J. A. Masucci, Z. Yan and W. Hageman, *Eur. J. Drug Metab. Pharmacokinet.*, 2004, **29**, 133–143.

69 R. S. Obach, *Drug Metab. Dispos.*, 1997, **25**, 1359–1369.

70 N. Tsamandouras, T. Kostrzewski, C. L. Stokes, L. G. Griffith, D. J. Hughes and M. Cirit, *J. Pharmacol. Exp. Ther.*, 2016, **360**, 95–105.

71 M. Pirmohamed, N. R. Kitteringham and B. K. Park, *Drug Saf.*, 1994, **11**, 114–144.

72 L. Di, B. Feng, T. C. Goosen, Y. Lai, S. J. Steyn, M. V. Varma and R. S. Obach, *Drug Metab. Dispos.*, 2013, **41**, 1975–1993.

73 J. Valentin, *Ann. ICRP*, 2002, **32**, 5–265.

74 R. D. Martin, D. J. Chivers, A. M. MacLarnon and C. M. Hladik, in *Size and Scaling in Primate Biology*, ed. W. L. Jungers, Springer US, Boston, MA, 1985, pp. 61–89, DOI: 10.1007/978-1-4899-3647-9_5.